# mmIDs Enter the 3rd Dimension: A Camera Inspired Broadbeam High-Gain Retrodirective Backscatter Tag

Charles A. Lynch III[#1], Genaro Soto-Valle[#], Jimmy Hester[*], Manos M. Tentzeris[#]
[#]ATHENA Lab, Georgia Institute of Technology, Atlanta, Georgia, USA
[*]Atheraxon, Atlanta, Georgia, USA
[1]clynch19@gatech.edu

2023 IEEE/MTT-S International Microwave Symposium - IMS 2023 | 979-8-3503-4764-7/23/$31.00 ©2023 IEEE | DOI: 10.1109/IMS37964.2023.10188156

***Abstract* — For the first time, the authors propose a mm-Wave (28 GHz) retrodirective backscatter system capable of large coverage in both azimuth and elevation directions. The structure, inspired by optical cameras, features a 3D-lens backed by an array of individual backscattering elements (pixels). First, the concept is presented. Then, the components of the system are described in detail, including the PTFE lens and the backscatter pixels array. Subsequently, the entire system is assembled and its combination of large azimuth/elevation coverage and differential Radar Cross Section (RCS) is measured, demonstrated, and compared to a lens-less system. Finally, the mmID is tested up to a range of 80 m to demonstrate its long-range potential. The mmID displays a −10 dB coverage of 0.736 sr about boresight, improving the angular coverage by 62 %, relative to the state of the art. This approach unlocks the deployment of dense battery-less 5G-connected mmID sensor swarms in smart city environments.**

***Keywords* — 5G, mm-Wave, mmID, 3D Lens, Long-range, IoT**

## I. Introduction

With recent developments and deployments of 5G/mm-Wave and radar technologies, unique opportunities to form battery-free ubiquitous sensing systems to provide real-time sensor-driven optimized Internet-of-Things (IoT) swarms serviced by the 5G infrastructure and autonomous vehicles have arisen. However, one of the draw-backs to utilizing 5G/mm-Wave is the large path losses incurred by these signals. To overcome this challenge, nodes can utilize large-gain phased-array based systems, required to steer and point the beam directly towards the interrogating gateway. However these phased-arrays typically consume at least a few watts [1] and are not suited for energy-autonomous densely-populated sensor node architectures. A technology that could, conceivably, enable ultra-low-power consumption—thereby reducing the need for a batteries which drive up maintenance and environmental costs—is backscatter communications. However, achieving large and steerable backscatter systems requires complex and power-hungry logic and phase-shifters. Fortunately, solutions providing the a priori impossible combination of high gain and angular coverage have been proposed in the form of passively retrodirective millimeter wave identification (mmID) structures [2], [3], [4], [5], [6].

Nevertheless, these designs are only operational over one angular dimension—usually, azimuth is chosen and, therefore, elevation coverage is poor. This problem is critical in typical urban areas where mmIDs and their 5G base-stations or autonomous interrogators can easily be placed at very different elevations and present quite oblique angles to each other. These also tend to be the conditions where the highest densities of such devices are likely to be installed.

The authors of this work propose, for the first time, a high-gain retrodirective mmID capable of broad coverage in all spatial directions. The structure is inspired by optical camera systems where a lens (or a series of lenses) focuses light received from given directions onto the pixels of a sensor. Here an optimized elliptical polymer 3D lens focalizes 28 GHz electromagnetic waves onto an array of individual backscattering pixels (as shown in Fig. 1) to form a large-gain mmID enabling high gain over a large solid angle, making for an orientation-agnostic mmID for ubiquitous wireless sensing applications. The remainder of this article is structured as follows: Section II describes each component of the ultra-long range orientation agnostic 3D lens-based mmID with their respective characterization. Having characterized the 3D Lens-based mmID, Section III presents a proof-of-concept demonstration of the ultra-long capabilities of the proposed system. Finally, Section IV concludes with highlights of the presented ultra-long range, orientation agnostic 3D lens-based mmID.

## II. Ultra-long range 3D Lens-based mmID

The proposed 5G/mm-Wave 3D lens-based mmID is comprised of two elements: the array of 17 cross-polarized backscattering pixels operating at 28 GHz, and the 3D elliptical lens that focalizes incoming electromagnetic radiation onto one of the 17 pixels, depending its angle of incidence. By combining these two components, the mmID enables high gain–and, thereby, ultra-long range interrogation ranges–while maintaining a spherically-symmetrical angular coverage of ±28 °.

### A. 5G/mm-Wave 3D Lens

The material selection of the 5G/mm-Wave lens is crucial to reduce the losses incurred by the incoming electromagnetic radiation during its travel through the lens. This is all the more crucial as the signal traverses the lens twice during the backscatter process. Therefore, the material selected for the lens was polytetrafluoroethylene (PTFE), a low-loss dielectric material with $\epsilon_r$= 2.1 and $\tan\delta$ =0.001, that has been used in various mm-Wave designs. For simplicity and cost-effectiveness at scale, an elliptical lens design was chosen. It was dimensioned, simulated, and optimized in CST

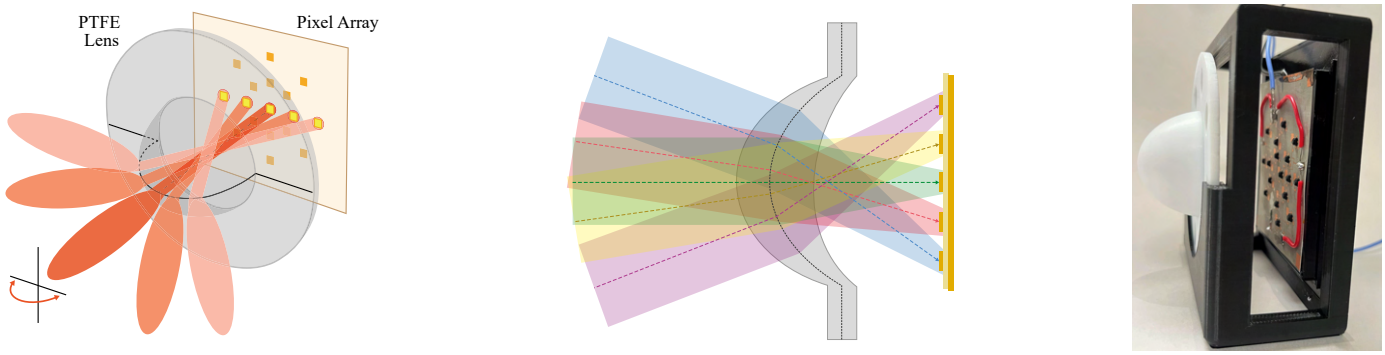


Fig. 1. (a) Diagram of the horizontal axis of coverage enabled by the 3D lens-based mmID. (b) Cross-sectional view of the 3D lens-based mmID; similar spherically-symmetrical coverage can be achieved in vertical, diagonal, and arbitrary orientation axis. (c) Fabricated proof-of-concept 3D lens-based mmID for ultra-long range 5G/mm-Wave IoT applications.

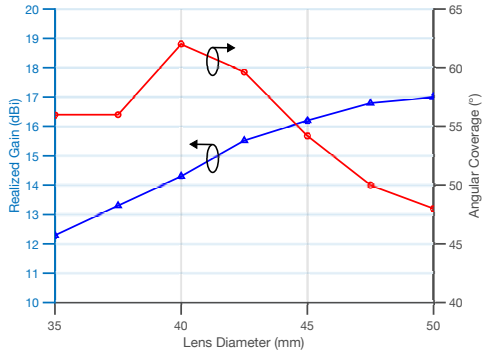


Fig. 2. Simulation results for the peak realized gain and 3 dB angular coverage of the system as a function of the diameter of the PTFE elliptical lens.

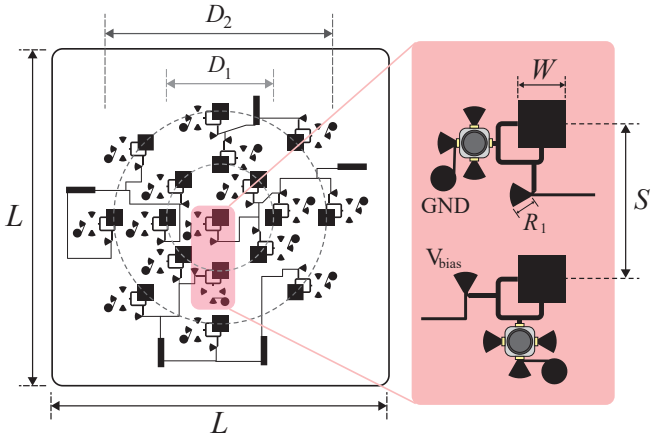


Fig. 3. 28 GHz cross-polarized mm-Wave backscattering elements ("pixels") layout with dimensions labeled $L = 60\,\text{mm}$, $D_1 = 19\,\text{mm}$, $D_2 = 38\,\text{mm}$ , $W = 2.9\,\text{mm}$, $S = 9.5\,\text{mm}$, and $R_1 = 1.22\,\text{mm}$.

Micro-wave studio. A focal length of 37 mm, providing a low profile to the tag, was set. The diameter of the lens was then swept (while preserving a constant displacement of 37 mm from the inner lens surface to the array plane) in the 35 mm to 50 mm range with 5 mm steps to quantify the influence of this parameter on both the 3 dB angular coverage and the gain of the system, yielding the plot displayed in Fig. 2.

As expected, the simulation results display an increasing peak realized gain with an increase in lens diameter, due to its increased aperture. However, the 3 dB angular coverage of provides a peak value of $\pm 31^\circ$ at 40 mm. Thus, a 40 mm diameter was chosen for the 3D elliptical lens allowing, for a significant gain while enabling a wide angular coverage, yielding a high detectability and a largely orientation agnostic behavior.

### B. *Cross-polarized Backscattering Array*

In order to enable the system with ultra-low-power communication capabilities—ideal for future 5G/mm-Wave-enabled IoT systems— backscatter communication was adopted and implemented via 17 cross-polarized backscattering elements (as shown in Fig. 3), radially distributed on a plane to provide a largely circularly symmetrical response to the mmID over its covered solid angle. Cross polarization of the received and backscattered signals has been shown to allow greater detectability by reducing cross talk at the reader [3], [4] and was, therefore, also adopted here. Each element consists of a cross-polarized 28 GHz square patch antenna, a multiple of $\frac{\lambda}{2}$ microstrip transmission line to match the input impedance of each feeding edge of the patch antennas, and a low-cost FET-based (CE3520K3 from CEL) switch; its dimension can be seen in the inset of Fig. 4. The switch further comprises radial stubs and a connection to the switched line, with appropriate dimensions to alternatively present a short or open parallel stub to it and to, therefore allow amplitude-based sub-carrier generation. Finally, two isolating $\frac{\lambda}{4}$ radial-stubs-based 28 GHz RF chokes, enabling baseband biasing between the gate and drain of the FET were added. The backscattering element was designed on a Rogers CLTE-MW ($\epsilon_r$= 3.03, $\tan\delta$ =0.0015) with a thickness of 0.254 mm. The FET switch was characterized for both biased and unbiased conditions, displaying more than 11 dB attenuation between its two states, as shown in the insertion loss plot of Fig. 4. Under biasing conditions, this ultra-low-cost switch consumes less than 1 µW while providing close-to-ideal properties for the modulation of the backscattered signal.

The backscattering element was then arrayed in two concentric circles of 19 mm and 38 mm in diameter—each

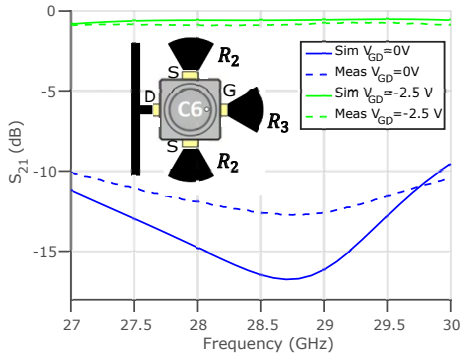


Fig. 4. Measured $S_{21}$ of the biased and unbiased states of the ultra-low-power FET-based switch and single element schematic (inset) with drain, gate, and source pins along with$R_2 = 1.14\,\mathrm{mm}$, and $R_3 = 1.55\,\mathrm{mm}$ labeled.

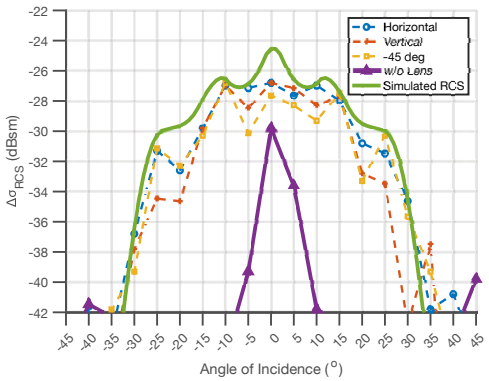


Fig. 5. Differential RCS of the 3D lens-based mmID for horizontal, vertical, $-45°$ angular cuts, and the backscattering array without the lens.

with eight patches distributed around each circle and a single element in the center, as displayed in Fig. 3. The orientation and the spacing of the arrays were optimized in simulation with the 3D lens in order to achieve continuous angular coverage over a $\pm 28°$ beamwidth around broadsight, in a circularly-symmetrical fashion.

### C. Characterization of the Integrated 3D Lens-based mmID

Having designed and fabricated both the 5G/mm-Wave 3D lens and backscattering array, the two subsystems were assembled together to form the mmID and its angular coverage was measured. The lens-based mmID was placed $1.4\,\mathrm{m}$ from two cross-polarized horn antennas and the power level of the backscattered sub-carrier was measured over angular sweeps of $-45°$ to $45°$ in steps of $5°$ with the 3D lens-based mmID placed on a stepper motor. This measurement was conducted for the horizontal, vertical, and the $-45°$ cut directions. Additionally, to verify the gain and improvement of utilizing this lens-based architecture, the backscattering array was also measured without the lens. The results for this angular characterization are displayed in Fig. 5 The results highlight the unmitigated superiority of the lens-based topology with an increase in the angular coverage from $10°$ to $56°$, while presenting a systematically superior Radar Cross Section (RCS). Thus, the proposed mmID architecture enables an orientation agnostic mmID that can be interrogated at ultra-long ranges with 5G/mm-Wave infrastructure over a wide solid angle in the top half hemisphere.

## III. Long Range Interrogation of 3D Lens-based mmID

Having characterized the properties of the proposed mmID, a long range demonstration was carried out. For interrogation, a $28.084\,\mathrm{GHz}$ continuous wave (CW) tone was generated with a 83640L signal generator and passed through the AHP2850-18-3024 power amplifier before, finally, being transmitted through a LB-180400-20-C-KF $20\,\mathrm{dBi}$ horn antenna oriented to transmit a vertical polarized radiation with a total effective isotropic radiated power (EIRP) of $36\,\mathrm{dBm}$. The signal was transmitted towards the mmID and modulated by at $800\,\mathrm{kHz}$ externally fed to the switches. The backscattered signal was then received with an identical horn antenna oriented in the horizontal polarization and passed through a RLNA26G40B $45\,\mathrm{dB}$ LNA—used to increase receiver sensitivity—and received on an Agilent 8565E spectrum analyzer. The reader sensitivity in $\mathrm{dBm}$ was calculated using $S_{Rx} = -174 + G_{LNA} + NF + 10\log_{10}(F_{Samp})$, where $G_{LNA}$, $NF$, and $F_{Samp}$ are the gain of the LNA in $\mathrm{dB}$, noise figure of the LNA in $\mathrm{dB}$, and sample rate in $\mathrm{Hz}$, respectively, and resulted in a sensitivity of $-105\,\mathrm{dBm}$. The mmID was placed directly boresight to the reader and moved in the $5\,\mathrm{m}$ to $80\,\mathrm{m}$ range in steps of $5\,\mathrm{m}$, with the power of the subcarrier recorded at each range. The experimental conditions of the $80\,\mathrm{m}$ measurement can be viewed in Fig.6. The measured received power, along a fitted empirical path loss exponent (EPLE)—measured as $n = 1.95$, matching well the expected value of 2 seen in outdoor environments and resulting in a $R^{-3.9}$ decaying power function for the two-way backscattering link—and the sensitivity of the proof-of-concept reader is displayed in Fig.7. The device could be readily interrogated at $80\,\mathrm{m}$, thereby demonstrating the ultra-long range of operation of the proposed system despite only using an EIRP of $36\,\mathrm{dBm}$. When operating with the maximum allotted EIRP at 5G/mm-Wave ($75\,\mathrm{dBm}$) and assuming a path loss exponent of $n = 2$, reading ranges of $2.5\,\mathrm{km}$ and $1.8\,\mathrm{km}$ are envisioned at boresight and at $28°$ angle of incidence to the mmID, respectively.

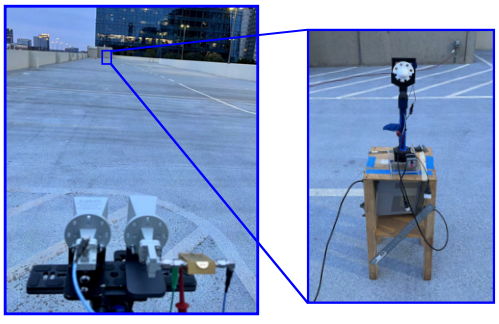

Fig. 6. Experimental setup for long-range demonstration of a proof-of-concept 5G/mm-Wave lens-based mmID at $80\,\mathrm{m}$.

Three metrics were used to evaluate and compare the proposed system (shown in Tab. 1) to other reflectarray-based

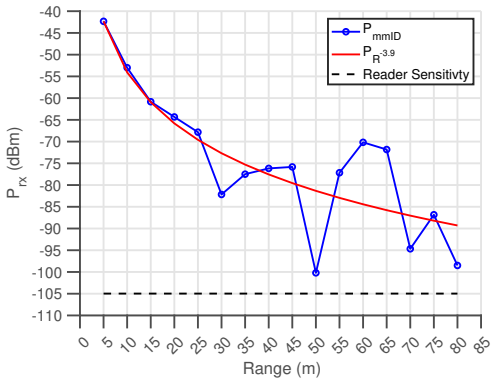


Fig. 7. Measured received power from the 3D lens-based mmID and its $R^{3.9}$ curve fitting as a function of range.

and lens-based mmIDs of the literature: the peak differential RCS, the azimuth and elevation angular coverage, and the total solid angle of coverage. The differential RCS can be expressed using the expression $\Delta\sigma_{RCS} = \lambda^2 G_{mmID}^2 |\Gamma_A - \Gamma_B| / 4\pi$, where $\lambda$, $G_{mmID}$, $\Gamma_A$, and $\Gamma_B$ are the wavelength of operation in meters, the gain of the mmID, and the reflection coefficients of the front-end in biased and unbiased states, respectively. This differential RCS was measured using a 6" metal sphere as a reference, as described in [5]. The solid angle metric was also determined by calculating the $-10\,\mathrm{dB}$ differential RCS angular beamwidth of each mmID in both $\phi$ and $\theta$. The proposed system displays a symmetrical response in both azimuth and elevation ("spherical symmetry")—a feat that no reported design has been able to achieve, while providing a detectability only attainable by large aperture or array systems. This ability to adequately backscatter signal impinging from oblique elevation as well as azimuth angles culminates in no less than a 62% increase in the solid angle that the proposed mmID features relative to state-of-the-art.

Table 1. Comparison of long-range reflectarray and lens-based RFID/mmID systems.

| Ref. | Freq. | $\Delta_{RCS}$ | Azim./Elev. Coverage | Solid Angle |
|---|---|---|---|---|
| [5] | 28 GHz | $-15.4\,\mathrm{dBsm}$ | $\pm 60\,^\circ/\pm 7.5\,^\circ$ | $0.453\,\mathrm{sr}$ |
| [3] | 28 GHz | $-29\,\mathrm{dBsm}$ | $\pm 60\,^\circ/\pm 7.5\,^\circ$ | $0.453\,\mathrm{sr}$ |
| This Work | 28 GHz | $-26.5\,\mathrm{dBsm}$ | $\pm 28\,^\circ/\pm 28\,^\circ$ | $0.736\,\mathrm{sr}$ |

## IV. Conclusion

For the first time, a proof-of-concept at 28 GHz 3D lens-based mmID is proposed for ultra-long range and wide azimuth and elevation backscatter coverage at mm-wave frequencies. The proof-of-concept ultra-low-power and compact mmID prototype featured an interrogation solid angle of $0.735\,\mathrm{sr}$ and provides an estimated peak differential RCS of $-26.50\,\mathrm{dBsm}$, making this system more than 62% superior to the state of the art in total angular coverage. Additionally, the high detectability of the mmID was highlighted through a proof-of-concept long range measurement measured out to $80\,\mathrm{m}$; utilizing the 5G maximum allotted $75\,\mathrm{dBm}$ EIRP, reading ranges of in excess of $2.5\,\mathrm{km}$ are envisioned. This approach solves a critical drawback of existing large-aperture mmID techniques and, finally, enables the ubiquitous implementation of mmID swarms in dense urban environments where oblique interrogations from 5G base-stations are likely to occur. This foundational effort sets the stage for further developments involving cascaded lens-based mmIDs to enable wider angular coverage by carefully correcting the aberrations of the 3D lens at high angles of incidence as well as the integration of metalenses for the z-axis miniaturization of low-profile smart-surface batteryless sensing systems for smart and energy-autonomous cities.

## References

[1] L. Dai, B. Wang, M. Wang, X. Yang, J. Tan, S. Bi, S. Xu, F. Yang, Z. Chen, M. D. Renzo, C.-B. Chae, and L. Hanzo, "Reconfigurable intelligent surface-based wireless communications: Antenna design, prototyping, and experimental results," *IEEE Access*, vol. 8, pp. 45 913–45 923, 2020.

[2] E. Sharp and M. Diab, "Van atta reflector array," *IRE Transactions on Antennas and Propagation*, vol. 8, no. 4, pp. 436–438, 1960.

[3] J. G. Hester and M. M. Tentzeris, "A mm-wave ultra-long-range energy-autonomous printed rfid-enabled van-atta wireless sensor: At the crossroads of 5g and iot," in *2017 IEEE MTT-S International Microwave Symposium (IMS)*, 2017, pp. 1557–1560.

[4] ——, "Inkjet-printed van-atta reflectarray sensors: A new paradigm for long-range chipless low cost ubiquitous smart skin sensors of the internet of things," in *2016 IEEE MTT-S International Microwave Symposium (IMS)*, 2016, pp. 1–4.

[5] A. Eid, J. G. D. Hester, and M. M. Tentzeris, "Rotman lens-based wide angular coverage and high-gain semipassive architecture for ultra-long range mm-wave rfids," *IEEE Antennas and Wireless Propagation Letters*, vol. 19, no. 11, pp. 1943–1947, 2020.

[6] C. A. Lynch, A. O. Adeyeye, A. Eid, J. Hester, and M. M. Tentzeris, "Ultra-long-range dual rotman lenses-based harmonic mmld's for 5g/mm-wave lot applications," in *2022 IEEE/MTT-S International Microwave Symposium - IMS 2022*, 2022, pp. 32–35.